Advances in Genomics and Genetics

Dovepress
open access to scientific and medical research

Open Access Full Text Article

ORIGINAL RESEARCH

MicroRNA activity profile in the ovarian cancer cell line OVCAR3 identifies a proapoptotic effect of miR-23a

This article was published in the following Dove Press journal:
Advances in Genomics and Genetics
23 October 2015
Number of times this article has been viewed

Vaagn Andikyan[1]
Gregory Mullokandov[2]
Judith Agudo[2]
Ravi Sachidanandam[3,4]
David Fishman[1]
Alessia Baccarini[2]
Brian D Brown[2,3]

[1]Department of Obstetrics, Gynecology and Reproductive Science, [2]Department of Genetics and Genomic Sciences, [3]Tisch Cancer Institute, [4]Department of Oncological Sciences, Icahn School of Medicine at Mount Sinai, New York, NY, USA

Introduction: Molecular profiling has revealed that many microRNAs (miRNAs) are highly expressed in ovarian carcinoma. However, it is not yet known which miRNAs are biologically active (ie, they suppress expression of a target gene) in ovarian cancer cells. Here we set out to determine the most active miRNAs in ovarian cancer cells.
Methods: We performed miRNA molecular profiling by quantitative polymerase chain reaction array, and measured miRNA activity using a library of sensor vectors for 291 different conserved miRNAs. We inhibited miR-23a activity using a lentiviral-based decoy, and measured the percentage of apoptotic cells by flow cytometry.
Results: Our miRNA activity profiling identified 54 active miRNAs in OVCAR3 cells, and found that over 150 miRNAs had no detectable activity. To study the function of an active miRNA, we selected miR-23a for further analysis. We inhibited miR-23a in OVCAR3 cells using a decoy vector, and found that there was decreased cell death compared to control (7.4%±1.4% versus 11.2%±0.5%; $P<0.05$) when the cells were treated with cisplatin. Moreover, the percentage of apoptotic cells was significantly lower in miR-23a inhibited cells compared to control (2.3%±0.4% versus 9.4%±2.6%; $P<0.05$).
Conclusion: This study identifies the active miRNAs in OVCAR3 cells, and suggests that miR-23a may help to regulate chemosensitivity of ovarian cancer cells.
Keywords: ovarian cancer, OVCAR3, microRNA profiling, miR-23a, apoptosis

Introduction

Ovarian cancer is the most lethal gynecological malignancy in the developed world, resulting in over 100,000 deaths per year.[1] The standard treatment of advanced ovarian cancer includes debulking surgery followed by adjuvant platinum based chemotherapy. Response to chemotherapy is one of the most important predictors of survival of patients with ovarian cancer.[2] Platinum-based compounds are considered the front-line chemotherapeutic agents for the treatment of patients with ovarian cancer.[3] Unfortunately, despite an initial clinical response to platinum-based chemotherapy, the majority of patients develop platinum resistance following treatment. Therefore, understanding the molecular pathways regulating response to platinum-based therapy and methods of overcoming platinum resistance should help improve the outcomes of ovarian cancer patients.

microRNAs (miRNAs) are a class of small non-coding RNAs that regulate gene expression at the post-transcriptional level.[4] The 20–23 nucleotide mature miRNA is derived from a longer RNA precursor that is transcribed from the genome, and assembles into a ribonucleoprotein complex called the RNA-induced silencing complex. miRNAs guide RNA-induced silencing complex to bind to the 3′ untranslated region of

Correspondence: Brian D Brown; Alessia Baccarini
Department of Genetics and Genomic Sciences, Icahn School of Medicine at Mount Sinai, 1470 Madison Avenue, New York, NY 10029, USA
Tel +1 212 824 8425; +1 212 824 9223
Email brian.brown@mssm.edu; alessia.baccarini@mssm.edu

submit your manuscript | www.dovepress.com
Dovepress
http://dx.doi.org/10.2147/AGG.S86586

target messenger RNAs (mRNAs) that are complementary to the miRNA sequence. This results in translational repression and a decrease in the stability of the bound mRNA, which ultimately leads to reduced levels of gene expression.

miRNAs have been found to play a role in almost all biological processes, and accumulating evidence indicates that the dysregulation of miRNA expression is fundamental to the pathophysiology of human cancers.[5] Numerous studies have demonstrated the important role of miRNAs as regulators of tumor phenotype. miRNAs control various steps in tumor progression including apoptosis, proliferation, differentiation, chemosensitivity, and metabolism. Several studies have reported the miRNA expression profiles of ovarian cancers.[6–8] For example, using a miRNA microarray, Yang et al found 36 miRNAs whose expression levels were dysregulated in ovarian tumors in comparison to normal ovarian cells.[8] The role of miRNAs in chemoresistance has also been demonstrated in several studies.[9,10] Li et al demonstrated in an ovarian cancer model that miR-128 could enhance cellular uptake of cisplatin and inhibits its efflux.[9] Zhao et al showed that miR-136 is deregulated in platinum-resistant ovarian cancer by affecting DNA repair and apoptosis.[10]

Measuring miRNA expression is generally used as the first step in identifying what may be the most relevant miRNAs to cell function. However, miRNA concentrations do not necessarily correlate with miRNA function.[4,11,12] Similar to mRNAs and proteins, miRNAs are subject to complex mechanisms of post-transcriptional regulation, which influences the miRNA's functionality even if it does not affect the miRNA's concentration.[12,13] For example, we and others have found that high concentrations of an miRNA's targets can saturate the miRNA, and reduce its regulatory activity.[11,13–17] It has also been shown that an miRNA can localize to subcellular compartments, and despite being expressed in the cell, it may not be able to contact its targets.[11,18] Thus, just like protein profiling is limited in its ability to predict protein activity, since many types of activating and inhibiting factors may not be readily detectable, miRNA profiling has similar limitations.

To address this issue, we have developed a novel approach, dubbed Sensor-seq, which uses a collection of 100s of sophisticated miRNA "sensor" vectors to quantitate the activity of each miRNA within a cell.[11] The collection is used as a pool, which makes the approach simple to perform. In contrast to molecular profiling, Sensor-seq provides a biological readout of an miRNA's regulatory potential. This can be used to identify the most functionally relevant and irrelevant miRNAs within cells, and to determine if miRNAs themselves are dysregulated. As a starting point to future studies in ovarian cancer, we set out to use Sensor-seq to identify the miRNA activity profile of the ovarian cancer model OVCAR3 cell line.

Materials and methods

Cell culture

OVCAR3 cells were grown in Roswell Park Memorial Institute medium with 20% fetal bovine serum and antibiotics (1% penicillin-streptomycin). Cells were maintained at 37°C in humidified condition with 5% CO_2. No ethics statement was required from the institutional review board for the use of this cell line.

Sensor-seq

We recently developed a library of miRNA sensors and a high-throughput methodology called Sensor-seq, for employing the sensor library.[11] The sensor is comprised of an integrating bidirectional lentiviral vector that coordinately expresses two reporter genes as distinct transcripts (Figure 1A). One reporter encodes a mutant NGFR gene, whereas the other encodes GFP linked to five tandem repeats of a perfectly complementary target site for a specific miRNA.[19] When cells are transduced with the vector, it stably integrates into the genome. Both reporters are expressed in cells, and can be detected by fluorescent activated cell sorting (FACS). However, if the cognate miRNA is active in the cells, it will bind to its target sites in the GFP transcript, and suppress its expression in a manner that is inversely proportional to the miRNA's activity (ie, high GFP expression indicates low miRNA activity, and low GFP expression indicates high miRNA activity). By using GFP as the reporter, we can measure the level of suppression mediated by an miRNA using FACS. This enables quantitation at single cell resolution, and the ability to flow sort the cells. NGFR was selected as the internal control because it can easily be detected by FACS using a fluorescent conjugated antibody.

After transduction of OVCAR3 cells with the miRNA sensor library, cells were FACS sorted on a FACS Vantage sorter (BD, Franklin Lakes, NJ, USA). The sorting and gate drawing were performed as previously described.[11] Genomic DNA was isolated from FACS sorted cells using a DNeasy Blood and Tissue Kit (Qiagen NV, Venlo, the Netherlands) as per manufacturer's recommendations. The extracted genomic DNA was prepared for deep sequencing as previously described (Figure 1).[11] Briefly, the region of the vector containing the miRNA target sites were polymerase chain reaction (PCR) amplified as a pool using primers outside the target sites and common

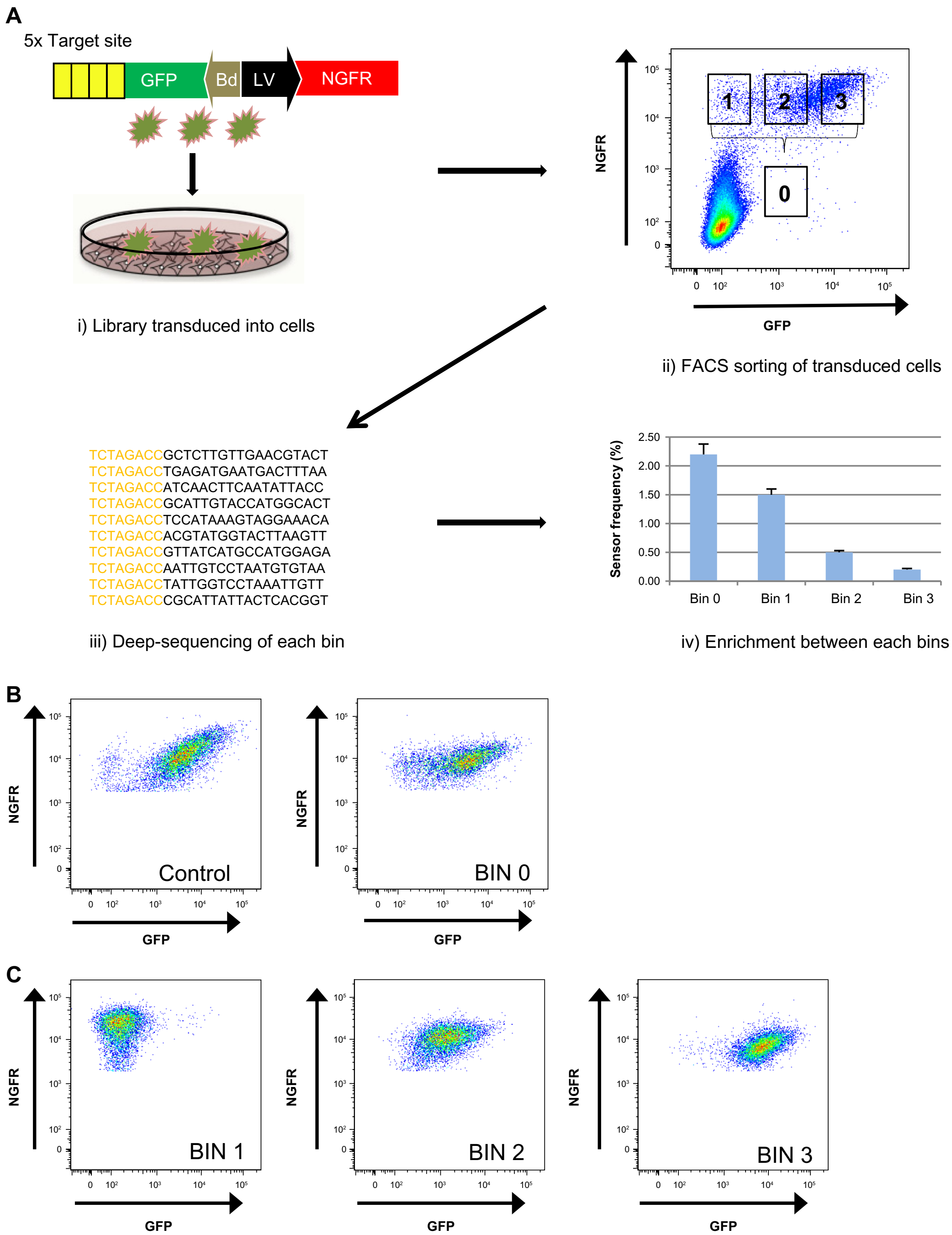

Figure 1 Sensor-seq analysis of OVCAR3 cells.
Notes: (**A**) The steps of the assay. (**B**) Control and Bin 0 in OVCAR3 cells. (**C**) Bin 1, 2, and 3 in OVCAR3. FACS plots are gated on NGFR+ cells (**B** and **C**).
Abbreviations: FACS, fluorescent activated cell sorting; BdLV, bidirectional lentiviral vector.

to all the sensors. Barcoded adapters were ligated to the PCR amplicons, and the corresponding libraries were subjected to deep-sequencing on the Illumina HiSeq platform (Illumina, Inc., San Diego, CA, USA). We obtained 2,000,000 reads per sample on average. The sequencing reads were mapped to the sensor library and the data were normalized by total read count. This provided a frequency for each sensor in each bin which was averaged between replicates.

miRNA PCR array

We performed real-time (RT)-PCR on OVCAR3 cells using RT^2 miRNA PCR array (Qiagen NV). The RT-PCR was performed as per manufacturer's recommendations.

Vector production and titration

Vectors were produced using lentiviral constructs as previously described.[20] Briefly, 293T-cells were used for vector production. Supernatant was collected after filtration through a 0.22 µm filter. Vectors were concentrated by ultracentrifugation and titers were estimated on 293T-cells by limiting dilution.

FACS

FACS of individual sensor vectors was performed using a BD Fortessa cell analyzer. Cells were analyzed for NGFR and GFP expression. We used either FlowJo (Tree Star, Inc., Ashland, OR, USA) or FCSExpress (De Novo Software, Los Angeles, CA, USA) to perform data analysis.

Cell death and apoptosis assays

OVCAR3 cells were transduced with individual miRNA decoys, plated in six-well plates, and treated with 4 µM of cisplatin for 24 hours. Dead cells were detected using 4′,6-diamidino-2-phenylindole (DAPI) nuclear staining. For apoptosis assays, the cells were evaluated using the Annexin V Apoptosis Detection Kit APC (eBioscience, Inc., San Diego, CA, USA). The percentage of dead and apoptotic cells was determined by FACS.

Quantitative real-time PCR analysis for miR-23a

Size fractionated total RNA from OVCAR3 cells was extracted using Qiazol reagent (Qiagen NV). For detection of miR-23a, 10 ng of size fractionated total RNA was reverse transcribed into complementary DNA using TaqMan MicroRNA Reverse Transcription Kit and the specific primers designed for miR-23a (Thermo Fisher Scientific, Waltham, MA, USA). The miR-23a level was measured by real-time PCR using TaqMan Universal PCR Master Mix (Thermo Fisher Scientific). The miRNA expression was normalized using the level of miR-16 as internal control.

Statistical analysis

Experiments were shown as the mean ± standard deviation. Student's *t*-test (two-tailed) was used to compare groups. Statistical significance was defined as $P<0.05$.

Results

miRNA molecular profile of OVCAR3 cells by quantitative PCR (qPCR)

To determine the miRNA profile of OVCAR3 cells, we measured the expression of 374 miRNAs in OVCAR3 cells by qPCR. The threshold cycle (CT) values were converted to arbitrary units (AU) on a linear scale using the deltaCT method with miR-16 serving as an internal calibrator. As has been previously reported for other cell lines, the miRNA profile fit a long-tail distribution with a relatively small number of miRNAs being highly expressed and the majority of miRNAs expressed at least ten fold lower (Figure 2).[21]

miRNA activity profile of OVCAR3 cells by Sensor-seq

Since the expression levels of an miRNA does not always correlate with its activity we performed Sensor-seq on the OVCAR3 cells to identify the most active miRNAs. Specifically, we transduced the cells with the miRNA sensor library at a low multiplicity of infection (<1) so that each cell was transduced with only a single sensor vector, as we have previously described.[11] Keeping the transduction rate below

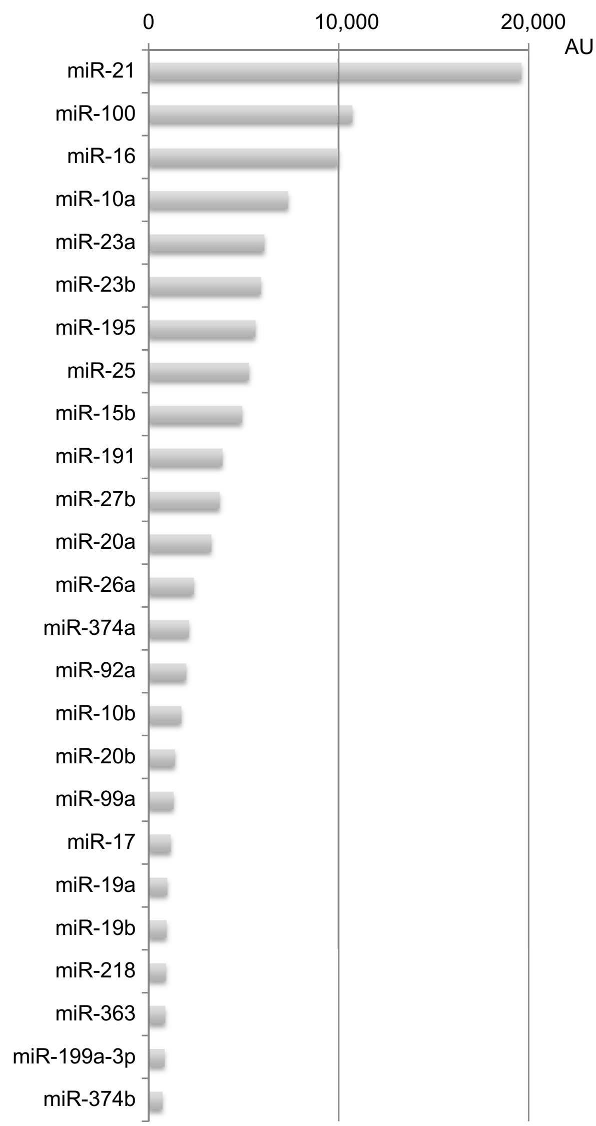

Figure 2 Quantitation of microRNA (miRNA) expression in OVCAR3 cells.
Notes: The top 25 highly expressed miRNAs (miR-16 10,000/2^ used for normalization); n=3.
Abbreviation: AU, arbitrary unit.

10% ensures that only a single sensor vector is integrated per cell. In our case we achieved transduction rates of 7.5% for OVCAR3 cells. As a control, cells were also transduced with the parent bidirectional lentiviral vector, which did not contain miRNA target sites in either reporter. GFP expression was different between cells transduced with the control or with the miRNA sensor library (Figure 1B). In OVCAR3 cells transduced with the parent vector, GFP and NGFR were similarly expressed. In contrast, while the majority of cells transduced with the sensor library were NGFR + GFP^{high} (non-active miRNAs) there were a significant number of cells that were NGFR+, but GFP^{low} (active miRNAs) or $GFP^{negative}$ (very active miRNAs). The suppression of GFP expression indicates these cells contain sensors for active miRNAs.

To identify the suppressed sensors, and thus the active miRNAs, we sorted the cells by FACS into three bins corresponding to $GFP^{negative}$ (Bin 1), GFP^{low} (Bin 2), and GFP^{high} (Bin 3) cells (Figure 1C). DNA was extracted from each group of cells, along with the total transduced population (Bin 0). We compared each sensor's frequency between bins and within the total population, (Figure 3). A significant enrichment in Bin 1 and/or Bin 2 (>1.5-fold, $P<0.05$), which contained $GFP^{negative}$ and GFP^{low} cells, indicated that the sensor was suppressed and, by inference, that the corresponding miRNA was active in these cells.

In OVCAR3 cells, and using this binning approach, 34 miRNAs were rated as very active, and 20 as active (Figure 3). We did not detect activity for 190 miRNAs (Table S1).

miR-23a is a very active miRNA in OVCAR3

To begin to understand the function of active miRNAs in OVCAR3 cells we selected one of the very active miRNAs, miR-23a, for further analysis. We selected miR-23a since its role and function has not been studied comprehensively in ovarian cancer. As a comparative control, we used a sensor for miR-142-3p, a hematopoietic-specific miRNA[22,23] that is not expressed in OVCAR3 cells, which means reporter expression can be considered maximal. The miR-23a sensor was enriched in Bin 1 and Bin 2 by 1.85- and 1.93-fold, respectively, relative to Bin 0 (Figure 4A and B). For miR-142-3p, there was no enrichment in either Bin 1 or Bin 2 compared to Bin 0; this was consistent with the fact that miR-142-3p was not detected in OVCAR3 cells by qPCR. To validate the Sensor-seq data we created an individual miRNA sensor for miR-23a and miR-142-3p. We transduced the OVCAR3 cells with each sensor and performed FACS analysis. As shown in Figure 4C, Sensor-seq data correlated well with individual sensors' FACS plots for both miR-23a and miR-142-3p in OVCAR3 cells.

Knockdown of miR-23a enhances cisplatin resistance in OVCAR3 cells

Several studies in hepatocellular and colon cancer have now demonstrated an association between miR-23a and chemoresistance.[24,25] We were therefore curious to investigate a possible relationship between miR-23a and platinum chemoresistance in OVCAR3 cells. We transduced OVCAR3 cells with an miR-23a decoy. This lentiviral-based vector integrates into the genome and stably inhibits miR-23a.[11] As a control, we transduced cells with a decoy for miR-142-3p which is not expressed or active in OVCAR3 cells. The miRNA decoys also express GFP. Following transduction the percentage of GFP-positive cells was >90% indicating that the vast majority of cells were expressing the decoy (Figure 5A). The decoy transcript inhibits its cognate miRNA by saturating it and by accelerating its rate of decay.[15] To assess the decoy effect, we extracted size fractionated total RNA from OVCAR3 cells transduced with miR-23a decoy and control cells (without miR-23a decoy) and measured miR-23a expression by qPCR. In cells expressing the miR-23a decoy there was a 2.5-fold reduction in miR-23a, indicating that the decoy was functioning and that miR-23a was suppressed (Figure 5B).

To determine if miR-23a has a role in chemoresistance, we treated OVCAR3 cells expressing the miR-23a decoy, or the control, with cisplatin (4 μM) for 24 hours. We assessed cell death by DAPI staining and FACS analysis. In the parent OVCAR3 cells or cells expressing the miR-142-3p decoy, there was essentially no difference in cells undergoing cell death in response to cisplatin (12.5%±2% and 11.2%±0.5%, respectively). By contrast, in OVCAR3 cells in which miR-23a was suppressed, only 7.4%±1.4% of the cells were DAPI-positive. The difference in the percentage of dead cells was statistically significant by Student's *t*-test ($P<0.05$) (Figure 5C). Overall these data demonstrate that OVCAR3 cells with miR-23a decoy had 1.7- and 1.5-fold decreased number of dead cells compared to controls (OVCAR3 parent cells and OVCAR3 cells expressing miR-142-3p decoy, respectively).

To further understand the role of miR-23a, we next assessed whether apoptosis was the cause of decreased cell death in OVCAR3 cells transduced with the miR-23a decoy. After cisplatin treatment we determined the frequency of apoptosis by Annexin V staining. In untransduced OVCAR3

A

microRNA	Bin0	Bin1	Bin2	Bin3
miR-106a	0.35%	5.94%	0.22%	0.09%
miR-106b	0.28%	0.95%	0.75%	0.04%
miR-10a	0.24%	0.54%	0.41%	0.02%
miR-125a-3p	0.11%	1.36%	0.04%	0.18%
miR-129-5p	0.04%	0.27%	0.02%	0.03%
miR-132	0.51%	6.08%	0.25%	0.37%
miR-145	0.06%	0.27%	0.01%	0.06%
miR-16	0.25%	0.68%	0.14%	0.03%
miR-181c	0.04%	0.15%	0.00%	0.05%
miR-18a	0.51%	7.07%	0.66%	0.06%
miR-196a	0.06%	0.19%	0.64%	0.02%
miR-19a	0.17%	1.04%	0.07%	0.01%
miR-19b	0.53%	1.95%	0.25%	0.06%
miR-200b	0.24%	0.46%	0.33%	0.37%
miR-20a	0.29%	3.21%	0.11%	0.10%
miR-20b	0.34%	0.98%	0.22%	0.06%
miR-214	0.89%	2.75%	3.22%	0.26%
miR-23a	0.33%	0.61%	0.63%	0.05%
miR-26a	0.09%	0.63%	0.03%	0.00%
miR-27b	0.37%	1.11%	0.30%	0.07%
miR-30a	0.39%	0.81%	0.34%	0.02%
miR-30d	0.41%	0.70%	1.76%	0.03%
miR-32	0.41%	3.54%	0.75%	0.03%
miR-335-3p	0.09%	0.41%	0.10%	0.01%
miR-335-5p	0.14%	1.12%	0.17%	0.00%
miR-363	0.39%	2.68%	0.55%	0.05%
miR-615-5p	0.00%	0.13%	0.00%	0.01%
miR-671-3p	0.03%	0.25%	0.06%	0.00%
miR-711	0.01%	0.15%	0.00%	0.00%
miR-761	0.45%	3.81%	0.06%	0.38%
miR-873	0.10%	0.35%	0.05%	0.06%
miR-876-5p	0.17%	5.12%	0.04%	0.15%
miR-92a	0.14%	2.49%	0.09%	0.01%
miR-93	0.09%	0.40%	0.05%	0.01%

B

microRNA	Bin0	Bin1	Bin2	Bin3
miR-103	0.56%	0.66%	1.35%	0.14%
miR-107	0.56%	0.36%	1.18%	0.14%
miR-1197	0.52%	0.23%	0.08%	0.22%
miR-1306	0.25%	0.01%	0.42%	0.31%
miR-146b	0.15%	0.02%	0.57%	0.03%
miR-191	0.47%	0.09%	1.42%	0.11%
miR-204	0.08%	0.00%	0.21%	0.09%
miR-210	0.21%	0.03%	0.76%	0.05%
miR-212	0.47%	0.04%	1.70%	0.29%
miR-221	0.18%	0.12%	0.36%	0.01%
miR-23b	0.29%	0.49%	0.65%	0.02%
miR-24	0.36%	0.03%	1.52%	0.20%
miR-27a	0.20%	0.48%	0.88%	0.03%
miR-29a	0.04%	0.02%	0.07%	0.01%
miR-30E	0.31%	0.35%	0.63%	0.07%
miR-342-3p	0.40%	0.15%	0.68%	0.15%
miR-425	0.98%	0.30%	2.54%	0.38%
miR-493	0.05%	0.00%	0.30%	0.01%
miR-99a	0.10%	0.10%	0.32%	0.01%
miR-99b	0.05%	0.00%	0.08%	0.01%

Figure 3 Analysis of target suppression in OVCAR3 cells by Sensor-seq.

Notes: (**A**) Sensor-seq profiles of highly active microRNAs (miRNAs) in OVCAR3 cells. High activity was defined by a significant enrichment (≥1.5-fold, $P<0.05$) in a sensor's frequency in Bin 1 (GFP-negative) compared to the sensor's overall frequency in Bin 0. Shown is the mean frequency for each sensor (n=3 biological replicates). (**B**) Sensor-seq profiles of moderately active miRNAs in OVCAR3 cells. Moderate activity was defined by a significant enrichment (≥1.5-fold, $P<0.05$) in a sensor's frequency in Bin 2 (GFP-low) compared to the sensor's overall frequency in Bin 0. Shown is the mean frequency for each sensor (n=3 biological replicates).

cells treated with cisplatin an average of 7.3%±3.1% of the cells were undergoing apoptosis (Annexin V positive). Similarly, 9.4%±2.6% of the OVCAR3 cells expressing the control decoy were apoptotic. By contrast, in miR-23a suppressed OVCAR3 cells only 2.3%±0.4% of the cells were undergoing apoptosis. The difference in apoptosis between the controls and miR-23a decoy cells was statistically significant ($P<0.05$) (Figure 5D). Taken together, OVCAR3 cells expressing miR-23a decoy demonstrated 3.2- and 4.1-fold decrease in amount of apoptotic cells compared to controls (OVCAR3 parent cells and OVCAR3 cells expressing miR-142-3p decoy, respectively).

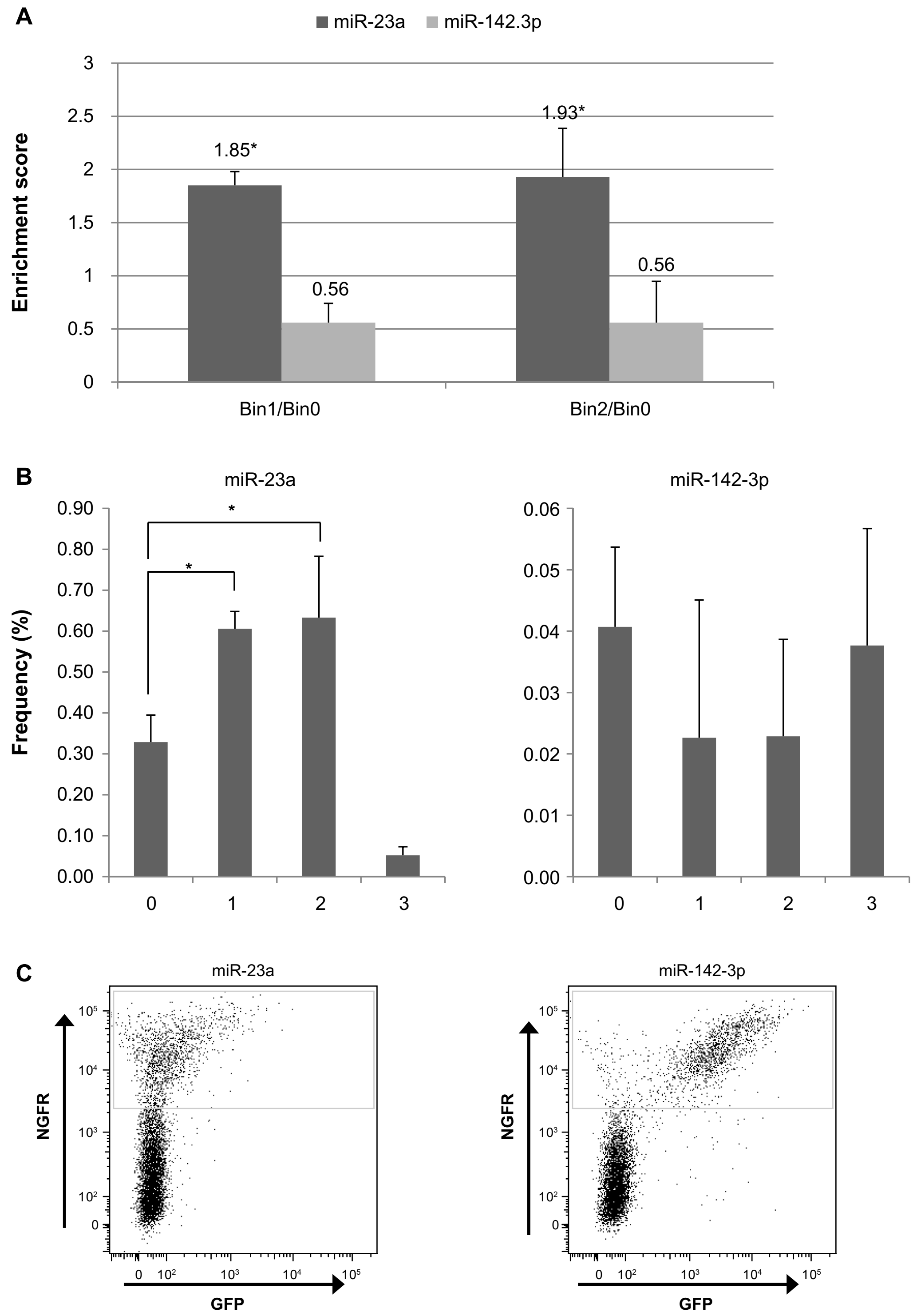

Figure 4 miR-23a and miR-142-3p in OVCAR3 cells.
Notes: (**A**) Enrichment scores. (**B**) miR frequencies. (**C**) Individual sensors in OVCAR3 cells. Error bars, standard deviation; n=3 (*$P<0.05$).

Discussion

In our study we demonstrated both the miRNA expression and activity profile of OVCAR3 cells. Based on activity profile we selected miR-23a for further analysis and demonstrated its proapoptotic effect.

We validated our findings of concordance between Sensor- seq and individual sensors by using miR-23a and miR-142-3p as an example. Our data demonstrate the enrichment scores and individual sensor FACS plots were concordant and, in general, support the approach. We

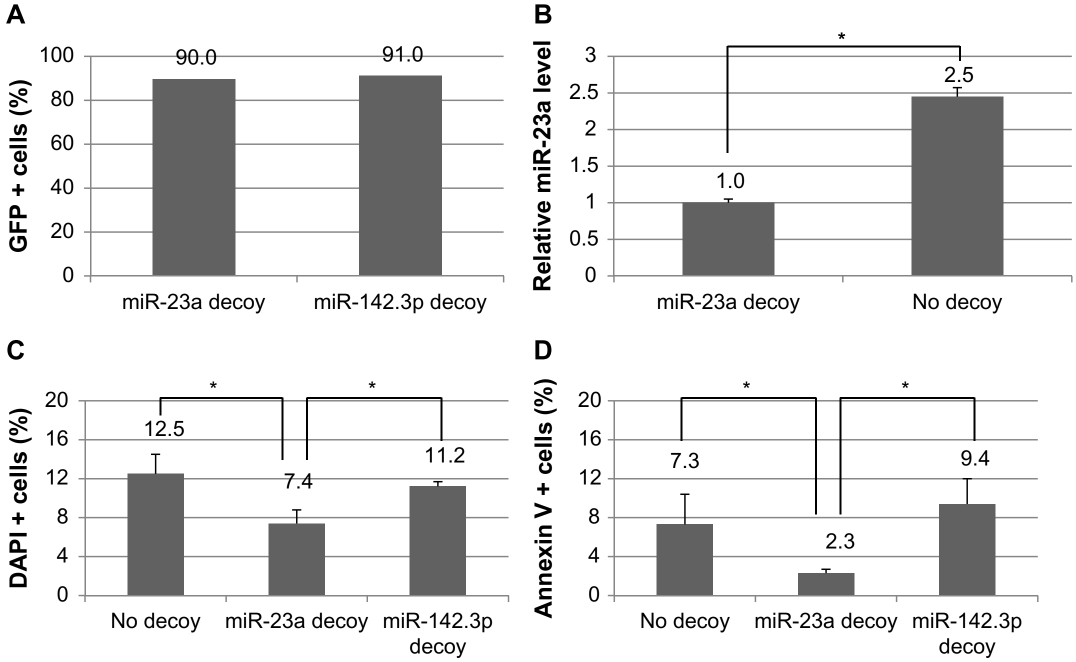

Figure 5 miR-23a in cell death and apoptosis.

Notes: (**A**) Percentage of GFP positive cells per individual decoy in OVCAR3 (by FACS); n=3. (**B**) Fold change of miR-23a expression after decoying. Error bars, standard deviation; n=3. (**C**) Percentage of cell death (4′,6-diamidino-2-phenylindole [DAPI] positive) per decoy after cisplatin treatment by FACS. Error bars, standard deviation; n=3. (**D**) Percentage of apoptotic cells (Annexin V positive) per decoy after cisplatin treatment by FACS. Error bars, standard deviation; n=3. $*P<0.05$.

Abbreviation: FACS, fluorescent activated cell sorting.

found that 34 miRNAs are highly active and 20 miRNAs are moderately active in OVCAR3 cells. As this is the first miRNA activity profile generated for an ovarian cancer cell line, we believe these data will provide a valuable resource for future studies of miRNA function in these cells. For example, one can use the activity profile to order candidate miRNAs for further functional analysis. Interestingly, while the overall trend was clear that more highly expressed miRNAs were more likely to be active, and lower expressed or undetectable miRNAs were less likely to be active, the miRNA expression levels obtained by qPCR and miRNA activity levels obtained by Sensor-seq did not correlate for all miRNAs. For example, miR-100 and miR-195 were highly expressed in OVCAR3 cells but there was little to no evidence of suppression for either sensor. This suggests that these miRNAs were inactive within the cell. This may be due to target-mediated titration or "sponging", as has been observed in other cell types, or another mechanism, such as miRNA nuclear localization.[4,26] Overall, these results provide evidence that miRNAs are subject to post-biogenesis control in OVCAR3 cells, and suggest that miRNA expression profiling alone cannot entirely predict an miRNA's behavior within the cell. Therefore, a combination of Sensor-seq and qPCR is necessary for identifying miRNAs that are likely to be functionally significant.

miRNA profiling provides a valuable tool to identify miRNAs that are aberrantly expressed and active in different cells including cancer cell lines. The role of several active miRNAs from our analysis have been reported previously in the context of OVCAR3 cell line. For example, miR-106a was studied by Li et al.[27] They demonstrated that miR-106a is involved in the development of drug resistance in OVCAR3 cells.[27] Using our activity profile in OVCAR3 future research can be conducted to investigate the role of active miRNAs in ovarian cancer.

We selected one of the very active miRNAs, miR-23a, to study its role in OVCAR3 cells. Previous studies have already highlighted a role for miR-23a in chemoresistance and apoptosis.[24,25] Wang et al demonstrated that overexpression of miR-23a potentiates human hepatocellular carcinoma cell to etoposide-induced cell death.[24] Shang et al demonstrated that miR-23a expression is negatively associated with 5-fluorouracil chemosensitivity in colon cancer cells in vitro.[25] Based on the available literature demonstrating the effect of miR-23a on chemoresistance and apoptosis we focused our attention on those properties of miR-23a. In this study we demonstrated the effect of miR-23a on chemotherapy-induced cell death and apoptosis. Here we show that suppression of miR-23a in OVCAR3 cells inhibits apoptosis and enhances chemoresistance. Thus, our data suggest that miR-23a plays a role as a proapoptotic agent in OVCAR3 cells and is therefore a candidate for playing the same role in ovarian tumors.

Acknowledgments

We thank the Flow Cytometry Core for technical assistance. This work was supported by NIH R33CA182377 and Human Frontiers RGP0009/2014 to BDB. JA was supported by the Robin Chemers Neustein Award, and GM was supported by NIH F30HL119039.

Disclosure

The authors report no conflicts of interest in this work.

References

1. Jemal A, Bray F, Center MM, Ferlay J, Ward E, Forman D. Global cancer statistics. *CA Cancer J Clin*. 2011;61(2):69–90.
2. Winter WE 3rd, Maxwell GL, Tian C, et al. Prognostic factors for stage III epithelial ovarian cancer: A gynecologic oncology group study. *J Clin Oncol*. 2007;25(24):3621–3627.
3. Siddik ZH. Cisplatin: mode of cytotoxic action and molecular basis of resistance. *Oncogene*. 2003;22(47):7265–7279.
4. Pasquinelli AE. MicroRNAs and their targets: recognition, regulation and an emerging reciprocal relationship. *Nat Rev Genet*. 2012;13(4):271–282.
5. Calin GA, Croce CM. MicroRNA signatures in human cancers. *Nat Rev Cancer*. 2006;6:857–866.
6. Parikh A, Lee C, Joseph P, et al. microRNA-181a has a critical role in ovarian cancer progression through the regulation of the epithelial-mesenchymal transition. *Nat Commun*. 2014;5:2977.
7. Yang D, Sun Y, Hu L, et al. Integrated analyses identify a master microRNA regulatory network for the mesenchymal subtype in serous ovarian cancer. *Cancer Cell*. 2013;23(2):186–199.
8. Yang H, Kong W, He L, et al. MicroRNA expression profiling in human ovarian cancer: MiR-214 induces cell survival and cisplatin resistance by targeting PTEN. *Cancer Res*. 2008;68(2):425–433.
9. Li B, Chen H, Wu N, Zhang WJ, Shang LX. Deregulation of miR-128 in ovarian cancer promotes cisplatin resistance. *Int J Gynecol Cancer*. 2014;24(8):1381–1388.
10. Zhao H, Liu S, Wang G, et al. Expression of miR-136 is associated with the primary cisplatin resistance of human epithelial ovarian cancer. *Oncol Rep*. 2015;33(2):591–598.
11. Mullokandov G, Baccarini A, Ruzo A, et al. High-throughput assessment of microRNA activity and function using microRNA sensor and decoy libraries. *Nat Methods*. 2012;9(8):840–846.
12. Tay Y, Kats L, Salmena L, et al. Coding-independent regulation of the tumor suppressor PTEN by competing endogenous mRNAs. *Cell*. 2011;147(2):344–357.
13. Cesana M, Cacchiarelli D, Legnini I, et al. A long noncoding RNA controls muscle differentiation by functioning as a competing endogenous RNA. *Cell*. 2011;147(2):358–369.
14. Salmena L, Poliseno L, Tay Y, Kats L, Pandolfi PP. A ceRNA hypothesis: the Rosetta Stone of a hidden RNA language? *Cell*. 2011;146(3):353–358.
15. Baccarini A, Chauhan H, Gardner TJ, Jayaprakash AD, Sachidanandam R, Brown BD. Kinetic analysis reveals the fate of a microRNA following target regulation in mammalian cells. *Curr Biol*. 2011;21(5):369–376.
16. Ameres SL et al. Target RNA-directed trimming and tailing of small silencing RNAs. *Science*. 2010;328(5985):1534–1539.
17. Franco-Zorrilla JM, Valli A, Todesco M, et al. Target mimicry provides a new mechanism for regulation of microRNA activity. *Nat Genet*. 2007;39:1033–1037.
18. Hwang HW, Wentzel EA, Mendell JT. A hexanucleotide element directs microRNA nuclear import. *Science*. 2007;315:97–100.
19. Brown BD, Gentner B, Cantore A, et al. Endogenous microRNA can be broadly exploited to regulate transgene expression according to tissue, lineage and differentiation state. *Nat Biotechnol*. 2007;25(12):1457–1467.
20. Agudo J, Ruzo A, Tung N, et al. The miR-126-VEGFR2 axis controls the innate response to pathogen-associated nucleic acids. *Nat Immunol*. 2014;15(1):54–62.
21. Brown BD, Naldini L. Exploiting and antagonizing microRNA regulation for therapeutic and experimental applications. *Nat Rev Genet*. 2009;10(8):578–585.
22. Chen CZ, Li L, Lodish HF, Bartel DP. MicroRNAs modulate hematopoietic lineage differentiation. *Science*. 2004;303(5654):83–86.
23. Brown BD, Venneri MA, Zingale A, Sergi Sergi L, Naldini L. Endogenous microRNA regulation suppresses transgene expression in hematopoietic lineages and enables stable gene transfer. *Nat Med*. 2006;12(5):585–591.
24. Wang N, Zhu M, Tsao SW, Man K, Zhang Z, Feng Y. MiR-23a-mediated inhibition of topoisomerase 1 expression potentiates cell response to etoposide in human hepatocellular carcinoma. *Mol Cancer*. 2013;12(1):119.
25. Shang J, Yang F, Wang Y, et al. MicroRNA-23a antisense enhances 5-fluorouracil chemosensitivity through APAF-1/caspase-9 apoptotic pathway in colorectal cancer cells. *J Cell Biochem*. 2014;115(4):772–784.
26. Jens M, Rajewsky N. Competition between target sites of regulators shapes post-transcriptional gene regulation. *Nat Rev Genet*. 2014;16:113–126.
27. Li H, Xu H, Shen H, Li H. microRNA-106a modulates cisplatin sensitivity by targeting PDCD4 in human ovarian cancer cells. *Oncol Lett*. 2014;7(1):183–188.

Supplementary material

Table S1 microRNAs with no detectable activity in OVCAR3 cells by Sensor-seq

miR-1	miR-139-5p	miR-216a	miR-367	miR-496
Let-7a	miR-140	miR-216b	miR-369-3p	miR-497
Let-7c	miR-141	miR-217	miR-369-5p	miR-499
miR-9	miR-142-3p	miR-219	miR-370	miR-500
miR-10b	miR-142-5p	miR-222	miR-376a	miR-501-3p
miR-15a	miR-144	miR-223	miR-376b	miR-501-5p
miR-15b	miR-146a	miR-224	miR-376c	miR-503
miR-17	miR-147	miR-296-3p	miR-377	miR-504
miR-21	miR-148b	miR-296-5p	miR-378	miR-532-3p
miR-22	miR-149	miR-298	miR-379	miR-532-5p
miR-26b	miR-150	miR-299	miR-381	miR-539
miR-28	miR-151-5p	miR-300	miR-382	miR-541
miR-29c	miR-152	miR-301a	miR-383	miR-542-3p
miR-31	miR-153	miR-301b	miR-409-3p	miR-542-5p
miR-34b-3p	miR-154	miR-302a	miR-409-5p	miR-544
miR-34b-5p	miR-181d	miR-302c	miR-410	miR-551b
miR-34c	miR-183	miR-323-3p	miR-411	miR-574-3p
miR-92b	miR-185	miR-323-5p	miR-421	miR-582-3p
miR-96	miR-186	miR-324-3p	miR-423-3p	miR-582-5p
miR-100	miR-187	miR-324-5p	miR-423-5p	miR-598
miR-105	miR-188-3p	miR-325	miR-429	miR-652
miR-122	miR-188-5p	miR-326	miR-431	miR-653
miR-124	miR-192	miR-329	miR-432	miR-654-3p
miR-125a-5p	miR-193b	miR-331-3p	miR-433	miR-654-5p
miR-125b-3p	miR-194	miR-331-5p	miR-448	miR-664
miR-126-3p	miR-195	miR-337-3p	miR-449a	miR-665
miR-126-5p	miR-196b	miR-337-5p	miR-450a-5p	miR-670
miR-127	miR-199a-3p	miR-338-3p	miR-451	miR-675-3p
miR-128	miR-199b	miR-338-5p	miR-452	miR-675-5p
miR-129-3p	miR-200a	miR-339-5p	miR-455	miR-708
miR-130a	miR-200c	miR-340-3p	miR-484	miR-720
miR-130b	miR-202-3p	miR-340-5p	miR-485	miR-744
miR-133a	miR-202-5p	miR-342-5p	miR-486	miR-759
miR-133b	miR-203	miR-345-3p	miR-487b	miR-760
miR-135a	miR-205	miR-345-5p	miR-488	miR-767
miR-135b	miR-208a	miR-361	miR-489	miR-875-3p
miR-138	miR-208b	miR-362-3p	miR-494	miR-875-5p
miR-139-3p	miR-211	miR-365	miR-495	miR-877